  Bull. Chem. Soc. Jpn., 64, 2887—2893 (1991)

Investigation of Ion and Solvent Transport Accompanying Redox Reactions of Polyvinylferrocene Films Using an in situ Electrochemical Quartz Crystal Microbalance Technique

Masaya MIZUNUMA,† Takeo OHSAKA,*,†† Hirohisa MIYAMOTO, and Noboru OYAMA*
Department of Applied Chemistry, Faculty of Technology, Tokyo University of Agriculture and Technology, 2-24-16 Naka-machi, Koganei, Tokyo 184
(Received May 14, 1991)

The in situ electrochemical quartz crystal microbalance (in situ EQCM) technique has been applied to study ion and solvent transport accompanying the redox reaction of polyvinylferrocene (PVF) film coated on quartz crystal electrodes in aqueous and acetonitrile media. The dependence of apparent formal potentials $(E^{f}_{poly})_{app}$ of the F_c°/F_c^{+} redox couple (F_c° and F_c^{+} represent the reduced and oxidized sites, respectively, in the PVF film) upon the concentration of supporting electrolyte has been also examined in comparison with those of solution-phase ferrocene derivatives. The PVF film is ideally permselective to ClO_4^- anion in both aqueous and acetonitrile media. The PVF oxidation (or reduction of polyvinylferricenium ion) in aqueous media is accompanied by the ingress (or egress) of one ClO_4^- ion per redox site and some solvent (ca. one H_2O per redox site). In $LiClO_4$ acetonitrile media, during the oxidation process ClO_4^- ion with some solvent inserts into the film and the reverse phenomenon occurs during the reduction process. The results demonstrate that a combination of the in situ EQCM measurement and the measurement of the dependence of $(E^{f}_{poly})_{app}$ on the concentration of supporting electrolyte makes possible to elucidate quantitatively the ion and/or solvent transport process across the polymer film/solution interface during the redox reaction.

Charge transport in electroactive polymer films, which are coated on electrode surfaces and are well-swollen with solvent/electrolyte, has been a subject of much interest in recent years from the viewpoint of the fundamental studies on the mechanism and kinetics of charge (electron and/or ion) transport as well as the potential applications (such as electrocatalysis, optical/electronic devices, sensors and energy storage) based on their interesting properties (e.g., electron transfer catalysis, ion permselectivity, redox conductivity and electrochromic property).[1] We have also been interested in this problem and have continued to conduct the kinetic and thermodynamic study of the homogeneous charge-transport process within polymer coatings for various types of redox polymer-coated electrode systems mainly using normal pulse voltammetry, potential-step chronoamperometry (chronocoulometry), AC impedance method and hydrodynamic voltammetry based on rotating disk electrodes.[2] A fruitful information about the charge transport has been obtained.[2] However, the role of electroinactive species (e.g., solvent and counter ions) in charge-transport processes can not be directly deduced using these electrochemical techniques.

The in situ electrochemical quartz crystal microbalance technique (in situ EQCM technique), which is based on the quartz crystal microbalance used in conjunction with electrochemistry, has recently received great attention as a highly useful technique capable of quantitatively measuring small mass changes (typically of the order of 10^{-9}—10^{-6} g) of electrode surfaces which occur as a result of electrochemical processes.[3] For some electroactive polymeric films (e.g., electropolymerized polymers and polymer complexes), mass changes, which occur upon electrochemical oxidation and reduction due to insertion and expulsion, respectively, of counter ions, coions and/or solvent into and out of the film phase, have been elucidated quantitatively using the in situ EQCM technique.[3,4]

In this paper, we report on the in situ EQCM responses for the redox reaction of polyvinylferrocene (PVF) film in aqueous and acetonitrile media, together with the comparison with the data reported by other workers for PVF films.[4b,c,h–j] The variation of apparent formal potential for the F_c°/F_c^{+} redox couple in the PVF film with the concentration of supporting electrolyte will be also examined in order to gain an additional insight into the mechanism of ion and solvent transport in PVF films. An analysis of apparent formal potential shifts of electroactive polymers as a function of the electrolyte concentration enables a quantitative estimation of concomitant changes in ion populations during their redox reactions.[4i,5]

Experimental

The electrochemical quartz crystal microbalance instrumentation and the experimental procedures are essentially similar to those employed in previous studies.[4a,d,e] The experiments reported here were run on a 5 MHz AT-cut quartz crystal (diameter: 13 mm, Toyo Kurafuto Ltd.) which are driven at their resonant frequency by a feedback osillator. Each side of the crystals was coated with Au (ca. 300 nm) by vaccum deposition, using Cr (ca. 2 nm) as an adhesion layer. One side of the crystal was further coated with PVF film (thickness is typically 150 nm) and used as the working electrode. A Pt wire and a sodium chloride saturated calomel electrode

† Present address: Materials & Electronic Devices Laboratory, Mitsubishi Electric Corp., Amagasaki, Hyogo 661.
†† Present address: Department of Electronic Chemistry, Graduate School at Nagatsuta, Tokyo Institute of Technology, 4259 Nagatsuta, Midori-ku, Yokohama 227.

(SSCE) were used as the counter and reference electrodes, respectively. The keyhole electrode design used is similar to that described in Ref. 6, with the piezoelectrically and electrochemically active areas being 63.6 and 47.8 mm^2,respectively. The crystal was affixed to the side of the cell via Teflon O-rings (Fig. 1). The mass change (Δm in g cm^{-2}) at the electrode surface could be estimated from the frequency change observed (Δf in Hz) according to Sauerbrey's equation;[7] $\Delta f = -C_f \Delta m$, with the proportionality constant C_f of 5.67×10^7 Hz cm^2 g^{-1}. The resonant frequency was measured using a Hewlett Packard 5334B frequency counter. EQCM data were obtained with the use of a computer-controlled apparatus.[4a]

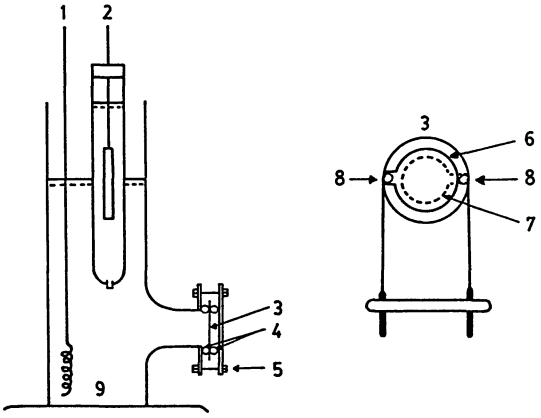

Fig. 1. A schematic depiction of the electrolyte cell and quartz crystal electrode used for in situ EQCM measurements. (1) counter electrode (Pt wire), (2) reference electrode, (3) quartz crystal (working electrode), (4) O-ring, (5) screw bolt/cap, (6) front electrode, (7) back electrode, (8) spring clip with attached lead, (9) glass cell.

The apparent formal potentials of the F_c^0/F_c^+ couple in the PVF film and the solution-phase ferrocenes in various concentrations of supporting electrolytes were obtained by cyclic voltammetry using basal-plane pyrolytic graphite (BPG, Union Carbide Co.) as a working electrode material. The reference and counter electrodes are the same as those employed in in situ EQCM experiments. The BPG disk electrodes (0.19 cm^2) were prepared and mounted into a glass tube with a heat-shrinkable polyolefin tube.

Polyvinylferrocene (PVF) was prepared according to Ref. 8. Adherent coatings of PVF were produced by transferring aliquots of a 0.1 wt% CH_2Cl_2 solution of PVF to the surface of a quartz crystal electrode and then evaporating the solvent at room temperature. The activity coefficients of ions were calculated according to the Debye-Hückel approximation.[9] All chemicals used were of reagent grade. Experiments were performed at room temperature (25±2 °C). All potentials were measured and were quoted with respect to the SSCE.

Results and Discussion

in situ EQCM Behavior of PVF Film in Aqueous Media. Figure 2 shows the typical results of in situ EQCM experiment on a PVF film-coated quartz crystal electrode in 0.26 M (1 M=1 mol dm^{-3}) $NaClO_4$ aqueous

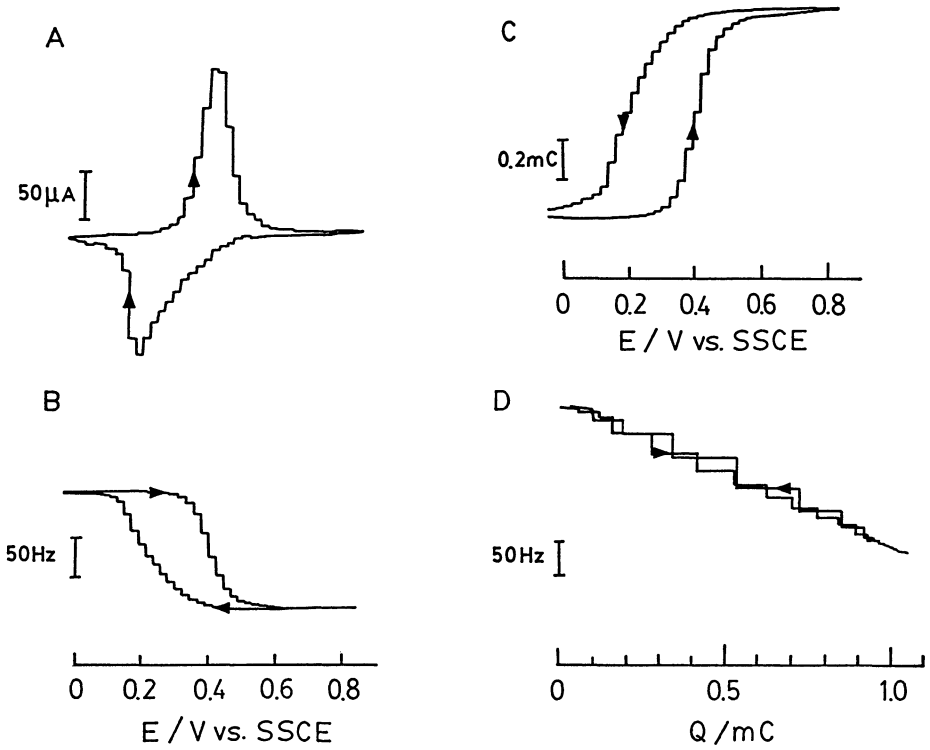

Fig. 2. (A) Current-potential, (B) frequency-potential, (C) charge-potential and (D)frequency-charge curves for a PVF film-coated quartz crystal electrode in 0.26 M $NaClO_4$ aqueous solution (pH 3.0). Amount of PVF coated on electrode: 17.3 μg cm^{-2}. Potential scan rate: 20 mV s^{-1}.

solution (pH 3.0). At first sight, we can see that the frequency change decreases during the oxidation process (i.e., the mass of the PVF film-coated electrode increases), while it increases during the reduction process (i.e., the mass decreases). In this case, the oscillator frequency completely returns to its initial value after the potential scan, indicating that the mass change of the PVF film accompanying its redox reaction is completely reversible on the time scale of the potential scan used (ca. 30—50 s). The half frequency change and half charge change potentials (denoted by $E_{1/2,f}$ and $E_{1/2,q}$, respectively, in this paper), at which the total frequency and charge changes, respectively, are half complete, may be used as measures of the ability of these quantities to respond to the applied potential program. At a scan rate of 20 mV s^{-1}, $E_{1/2,f}$ and $E_{1/2,q}$ are almost the same values of ca. 0.20 and 0.40 V for the negative and positive scans, respectively. This fact demonstrates that the mass transport process and electron transfer process occur simultaneously at the scan rate used, because the frequency change can be linearly correlated to the mass change according to the Sauerbrey's equation. From Fig. 2D, it is obvious that the frequency change vs. charge plots are almost linear for both anodic and cathodic processes and the slopes for both processes are almost the same (1.48×10^5 Hz C^{-1}). The increase in mass per mole of redox sites of PVF film, i.e., the molar mass equivalent (M_{eq}), could be determined to be 119 g mol^{-1} using the slopes of the Δf vs. Q plots. The physical significance of the M_{eq} obtained will be mentioned below.

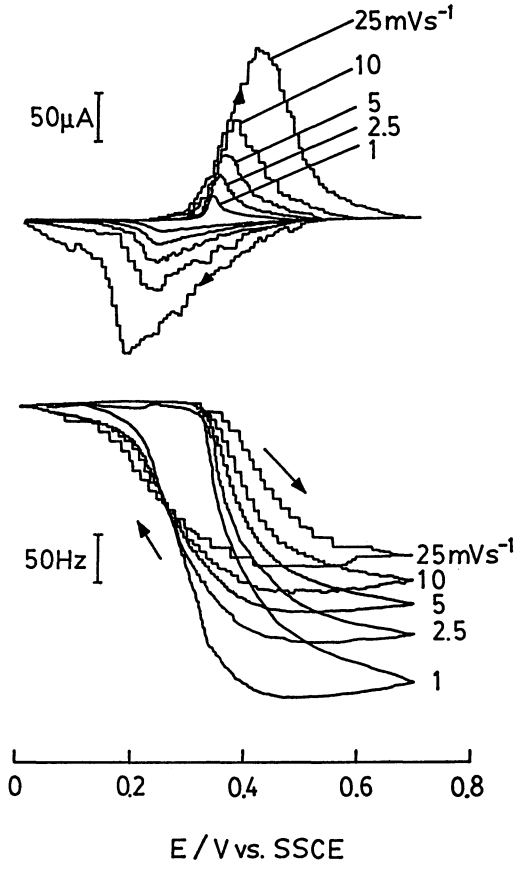

Fig. 3. Typical cyclic voltammetric and frequency-potential curves for a PVF film-coated quartz crystal electrode in 0.2 M $NaClO_4$ aqueous solution (pH 3.0) at various potential scan rates. Amount of PVF coated on electrode: 17.3 μg cm^{-2}.

Figure 3 shows typical cyclic voltammetric and frequency-potential curves for the PVF film-coated quartz crystal electrode in 0.2 M $NaClO_4$ aqueous solution (pH 3.0) at various potential scan rates of 1 to 25 mV s^{-1}. The frequency change response accompanying the redox reaction is essentially the same as that mentioned above (Fig. 2). In addition, we can see that the difference in frequency change between the oxidized and reduced states is larger at slower potential scan rate. This is qualitatively understood by considering that the number (Γ) of the redox sites in the film oxidized (or reduced) during a given potential scanning is proportional to the amount (Q) of charge passed during the period and that the oxidation (or reduction) process will require, for charge neutrality, concurrent ingress (or egress) of anion into (or out of) the film matrix. The measured values of Q, Γ, and Δf at various scan rates are summarized in Table 1, together with the calculated ones of Δm and M_{eq}. Γ and Δm increases, as expected, with decreasing potential scan rate. However, the M_{eq} values are almost constant ((123±4) g mol^{-1}). If ClO_4^- anion were the only mobile species to be transferred, the resultant value would be 99.5 g mol^{-1}. Thus, the fact that the M_{eq} obtained is larger than 99.5 g mol^{-1} may suggest the PVF oxidation (or PVF^+ reduction) is accompanied by the ingress (or egress) of one ClO_4^- ion per redox site and some solvent (ca. one H_2O per redox site), being in a qualitative agreement with the results previously reported for PVF films.[4b,h,i]

Dependence of Apparent Formal Potential on Electrolyte Concentration. When the PVF film is ideally permselective to ClO_4^- anion, the apparent formal potential ($(E^f_{poly,H_2O})_{app}$) of the F_c°/F_c^+ redox couple (F_c° and F_c^+ represent the reduced and oxidized sites, respectively, in the PVF film) in aqueous solutions could be expected to obey the following equation.

Table 1. in situ EQCM Data of PVF Film in Aqueous $NaClO_4$ Media[a)]

v[b)]	Q	$10^8\cdot\Gamma$	$-\Delta f$	$10^6\cdot\Delta m$	M_{eq}
mV s^{-1}	mC	mol cm^{-2}	Hz	g cm^{-2}	g mol^{-1}
1	1.83	3.97	286	5.03	126
2.5	1.51	3.28	235	4.13	126
5	1.36	2.95	207	3.64	123
10	1.19	2.58	181	3.18	123
25	1.06	2.30	155	2.73	119

a) Concentration of $NaClO_4$: 0.2 M. Thickness of PVF film in dry state: 150 nm. Electrochemically active area: 47.8 mm^2. See the text for the definitions of Q, Γ, Δf, Δm, and M_{eq}. b) Potential scan rate.

$$(E^{f}_{poly,H_2O})_{app} = E^{\circ}_{poly,H_2O} + E_j - \frac{RT}{F}\ln\frac{f^{F_c^{\circ}}_{poly,H_2O}}{f^{F_c^{+}}_{poly,H_2O}} - \frac{RT}{F}\ln a_{(ClO_4^-)_{soln,H_2O}}, \quad (1)$$

where $(E^{f}_{poly,H_2O})_{app}$ (vs. SSCE) was taken as the average of the anodic and cathodic peak potentials of the cyclic voltammograms for the F_c°/F_c^{+} couple obtained at the PVF film-coated BPG electrode in $NaClO_4$ aqueous solutions (0.02—2.0 M), E°_{poly,H_2O} is the standard potential of the F_c°/F_c^{+} couple in the aqueous solutions used here, E_j denotes the liquid junction potential at SSCE (aq): $NaClO_4$ (0.02—2.0 M, aq), $f^{F_c^{+}}_{poly,H_2O}$ and $f^{F_c^{\circ}}_{poly,H_2O}$ are the activity coefficients of the F_c^{+} and F_c° redox sites, respectively and $a_{(ClO_4^-)_{soln,H_2O}}$ is the activity of ClO_4^- ion in $NaClO_4$ aqueous solutions. The last term on the right-hand side of Eq. 1 represents "Donnan potential" present at the PVF film/solution interface. On the other hand, the apparent formal potential ($(E^{f}_{soln,H_2O})_{app}$) for the monomeric ferrocene derivative (i.e., ferrocenylmethyl(trimethylammonium), F_c–N^+) dissolved in the same aqueous solutions can be written as follows:

$$(E^{f}_{soln,H_2O})_{app} = E^{\circ}_{soln,H_2O} + E_j - \frac{RT}{F}\ln\frac{f^{F_c\text{-}N^+}_{soln,H_2O}}{f^{F_c\text{-}N^{2+}}_{soln,H_2O}}, \quad (2)$$

where $(E^{f}_{soln,H_2O})_{app}$ was measured with respect to the SSCE, E°_{soln,H_2O} is the standard potential of the F_c–N^+/F_c–N^{2+} couple, and $f^{F_c\text{-}N^{2+}}_{soln,H_2O}$ and $f^{F_c\text{-}N^+}_{soln,H_2O}$ are the activity coefficients of F_c–N^+ and F_c–N^{2+}, respectively.

As can be seen from Fig. 4, the polts of $(E^{f}_{poly,H_2O})_{app}$ vs. $\log a_{(ClO_4^-)_{soln,H_2O}}$ and $(E^{f}_{soln,H_2O})_{app}$ vs. $\log a_{(ClO_4^-)_{soln,H_2O}}$ are linear in the examined range of $a_{(ClO_4^-)_{soln,H_2O}}$ with slopes of −62 and −5 mV per decade in ClO_4^- activity, respectively. Thus, the difference ($\Delta(E^{f}_{H_2O})_{app}$) between $(E^{f}_{poly,H_2O})_{app}$ and $(E^{f}_{soln,H_2O})_{app}$ can be expressed by

$$\Delta(E^{f}_{H_2O})_{app} = (E^{\circ}_{poly,H_2O} - E^{\circ}_{soln,H_2O}) - \left(\frac{RT}{F}\ln\frac{f^{F_c^{\circ}}_{poly,H_2O}}{f^{F_c^{+}}_{poly,H_2O}} - \frac{RT}{F}\ln\frac{f^{F_c\text{-}N^+}_{soln,H_2O}}{f^{F_c\text{-}N^{2+}}_{soln,H_2O}}\right) - \frac{RT}{F}\ln a_{(ClO_4^-)_{soln,H_2O}}. \quad (3)$$

This enables us to evaluate the dependence of the formal potential difference on the electrolyte activity without knowing the dependence of E_j on the electrolyte activity under the condition that the second term on the right-hand side of Eq. 3 can be assumed as a constant in the examined range of $a_{(ClO_4^-)_{soln,H_2O}}$.[11] Based on its definition, the term $(E^{\circ}_{poly,H_2O} - E^{\circ}_{soln,H_2O})$ is independent of $a_{(ClO_4^-)_{soln,H_2O}}$. If the above condition is fulfilled, the slope of $\Delta(E^{f}_{H_2O})_{app}$ vs. $\log a_{(ClO_4^-)_{soln,H_2O}}$ plot can be expected to be −59 mV per decade in ClO_4^- activity at 25 °C. The actually obtained value is −57 mV per decade. This fact strongly suggests the permselective movement of ClO_4^- anions to the PVF film in order to maintain electroneutrality in agreement with the above-mentioned in situ EQCM results. There is no evidence for cation population changes during the redox reaction under the experimental conditions employed in this study.

According to the results obtained, the following reaction mechanism can be postulated for the PVF film reaction:

$$(F_c^{\circ}, nH_2O)_{poly} + (ClO_4^-)_{soln} + m(H_2O)_{soln} \rightleftarrows (F_c^{+}\cdot ClO_4^-, (n+m)H_2O)_{poly} + e^-, \quad (4)$$

where the subscripts refer to the polymer film (poly) or supporting electrolyte solution (soln). Note that the values of the coefficients m and n are not necessarily integers, as pointed out recently.[10] The ion and solvent transport that accompanies the redox reaction of PVF film coated on the electrode is depicted schematically in Fig. 5.

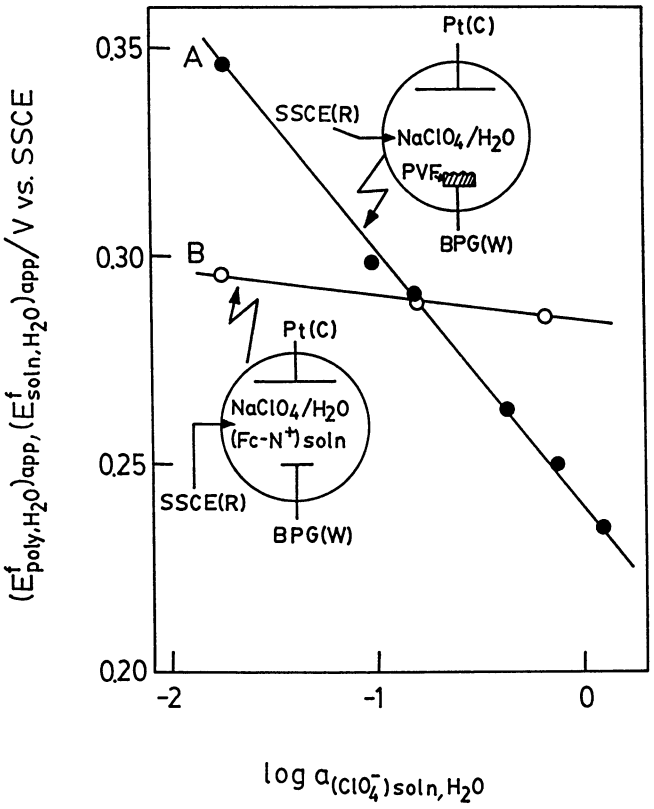

Fig. 4. Apparent formal potentials of (A) the F_c°/F_c^{+} couple in the PVF film and (B) the solution-phase F_c-N^+/F_c-N^{2+} couple as a function of the activity of the $NaClO_4$ supporting electrolyte. Amount of PVF coated on BPG electrode: 21.5 μg cm^{-2}. Concentration of F_c-N^+ in solution: 1 mM. The insets schematically represent the three-electrode systems employed to examine the dependence of $(E^{f}_{poly,H_2O})_{app}$ and $(E^{f}_{soln,H_2O})_{app}$ upon $\log a_{(ClO_4^-)_{soln,H_2O}}$.
W: working electrode, R: reference electrode, C: counter electrode.

in situ EQCM Behavior of PVF Film and Dependence of Formal Potential on Electrolyte Concentration in Acetonitrile Media. Figure 6 shows in situ EQCM data obtained on potential cycling (at 10 mV s^{-1}) of the

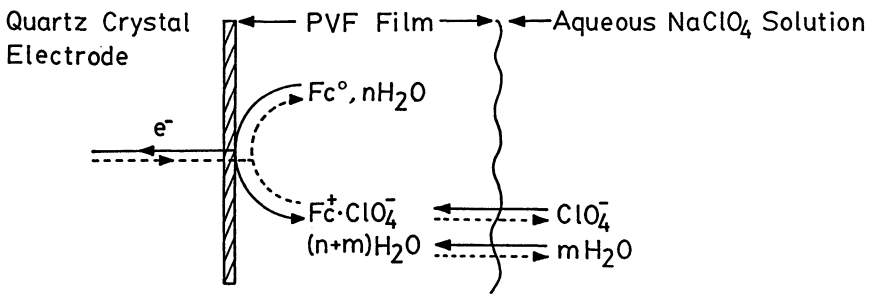

Fig. 5. Schematic representation of the ion and solvent transport that accompanies the redox reaction of the PVF film on the electrode in aqueous $NaClO_4$ solutions. F_c^+ and F_c° represent the oxidized and reduced sites, respectively, in the PVF film.
(——): oxidation process, (– – –): reduction process.

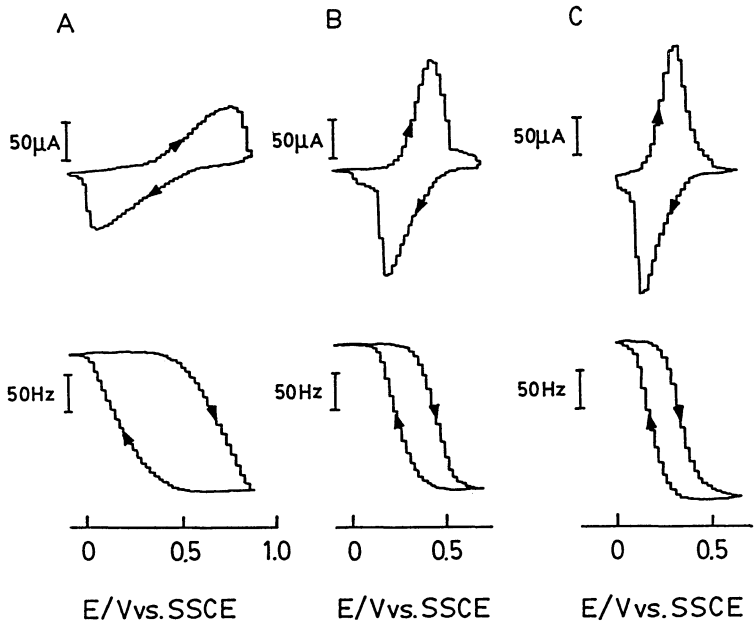

Fig. 6. Cyclic voltammetric and frequency-potential curves for a PVF film-coated quartz crystal electrode in acetonitrile solutions containing various concentrations of $LiClO_4$. Amount of PVF coated on electrode: 21.5 $\mu g\,cm^{-2}$. Concentration of $LiClO_4$ in acetonitrile electrolyte solutions: (A) 0.02, (B) 0.20, and (C) 2.0 M. Potential scan rate: 10 $mV\,s^{-1}$.

Table 2. in situ EQCM Data of PVF Film in Acetonitrile $LiClO_4$ Media[a)]

$C^{b)}$	$v^{c)}$	Q	$10^8 \cdot \Gamma$	$-\Delta f$	$10^6 \cdot \Delta m$	M_{eq}
M	$mV\,s^{-1}$	mC	$mol\,cm^{-2}$	Hz	$g\,cm^{-2}$	$g\,mol^{-1}$
0.02	20	1.29	2.80	176	3.09	110
	10	1.28	2.78	168	2.96	106
0.20	20	1.41	3.06	184	3.24	106
	10	1.45	3.15	192	3.37	107
0.63	20	1.44	3.12	187	3.29	105
	10	1.42	3.08	183	3.22	105
1.20	20	1.44	3.12	200	3.52	113

a) Thickness of PVF film in dry state: 150 nm. Electrochemically active area: 47.8 mm^2. See the text for the definitions of Q, Γ, Δf, Δm, and M_{eq}. b) Concentration of $LiClO_4$. c) Potential scan rate.

PVF film in acetonitrile solutions containing various concentrations of $LiClO_4$. The frequency change (and so the mass change) of the film-coated electrode accompanying its redox reaction seems reversible, regardless of the concentration of $LiClO_4$. Note that the large potential difference between the anodic and cathodic peak potentials of voltammogram A, compared with those of voltammograms B and C, may originate from the significant *iR* drop effect due to the low concentration of the supporting electrolyte used. It was also found that for a given concentration of $LiClO_4$ $E_{1/2,f}$ and $E_{1/2,q}$ coincide within 5 mV. The mass transport process and electron transfer process are thus thought to occur simultaneously.

Table 2 contains the quantitative results concerning the charge transport, estimated from the data such as those shown in Fig. 6. The values of molar mass equivalent M_{eq} are almost the same ((109±4) g mol^{-1}), regardless of the concentration of $LiClO_4$ supporting electrolyte. However, these values are essentially larger than that (99.5 g mol^{-1}) expected when ClO_4^- is the only mobile species to be transferred. As in the case of the above-mentioned $H_2O/NaClO_4$ system, the dependence of the formal potential on the activity of

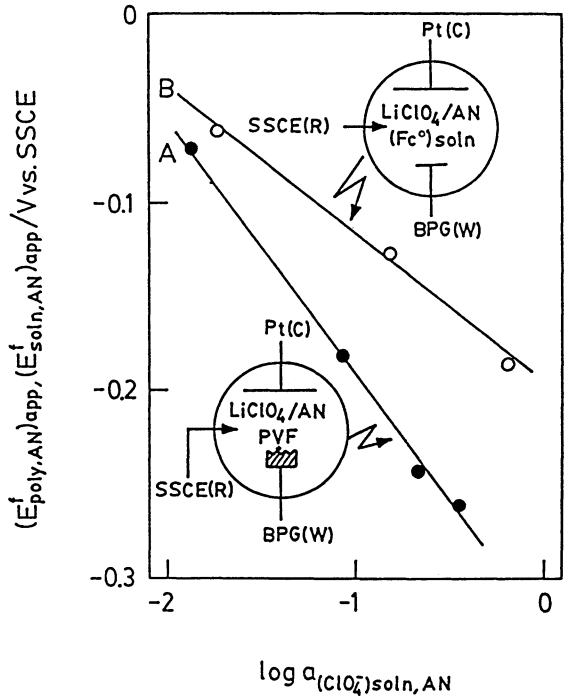

Fig. 7. Apparent formal potentials of (A) the Fc°/Fc^+ couple in the PVF film and (B) the solution-phase Fc°/Fc^+ couple as a function of the activity of the $LiClO_4$ supporting electrolyte. Amount of PVF coated on BPG electrode: 21.5 μg cm^{-2}. Concentration of ferrocene (Fc°) in solution: 1 mM. The insets schematically represent the three-electrode systems employed to examine the dependence of $(E^f_{poly,AN})_{app}$ and $(E^f_{soln,AN})_{app}$ upon $\log a_{(ClO_4^-)_{soln,AN}}$.
W: working electrode, R: reference electrode, C: counter electrode.

ClO_4^- in acetonitrile (AN) solutions was also examined. The results are shown in Fig. 7. Here, the apparent formal potentials ($(E^f_{poly,AN})_{app}$ and $(E^f_{soln,AN})_{app}$) for the Fc°/Fc^+ couple in the PVF film and the solution-phase ferrocene/ferricinium couple in acetonitrile solutions can be represented by the Nernstian expression:

$$(E^f_{poly,AN})_{app} = E^\circ_{poly,AN} + E_j' - \frac{RT}{F}\ln\frac{f^{Fc^\circ}_{poly,AN}}{f^{Fc^+}_{poly,AN}} - \frac{RT}{F}\ln a_{(ClO_4^-)_{soln,AN}}, \quad (5)$$

$$(E^f_{soln,AN})_{app} = E^\circ_{soln,AN} + E_j' - \frac{RT}{F}\ln\frac{f^{Fc^\circ}_{soln,AN}}{f^{Fc^+}_{soln,AN}}, \quad (6)$$

where $(E^f_{poly,AN})_{app}$ and $(E^f_{soln,AN})_{app}$ were measured with respect to the SSCE, E_j' is the liquid junction potential between SSCE (aq) and $LiClO_4$ (0.02—1.0 M, AN), and the other terms correspond to those of the acetonitrile solution system in place of the aqueous solution system (Eqs. 1 and 2). The plot of $(E^f_{poly,AN})_{app}$ (or $(E^f_{soln,AN})_{app}$) vs. $\log a_{(ClO_4^-)_{soln,AN}}$ gave the straight line with slope of −136 (or −78) mV per decade in ClO_4^- activity in the examined range of $a_{(ClO_4^-)_{soln,AN}}$ (see Fig. 7). Thus, one can obtain the linear relation between $\Delta(E^f_{AN})_{app}$ ($=(E^f_{poly,AN})_{app}-(E^f_{soln,AN})_{app}$) and $a_{(ClO_4^-)_{soln,AN}}$. In this case, the slope of $\Delta(E^f_{AN})_{app}$ vs. $\log a_{(ClO_4^-)_{soln,AN}}$ plot is −58 mV per decade in $a_{(ClO_4^-)_{soln,AN}}$ which almost coincides with that (−59 mV per decade) expected for the case where the PVF film is ideally permselective to ClO_4^- anion and the dependences of the activity coefficient terms for the polymer film and solution-phase systems i.e.,

$$\frac{RT}{F}\ln\frac{f^{Fc^\circ}_{poly,AN}}{f^{Fc^+}_{poly,AN}} \quad \text{and} \quad \frac{RT}{F}\ln\frac{f^{Fc^\circ}_{soln,AN}}{f^{Fc^+}_{soln,AN}}$$

upon the activity of ClO_4^- are the same.

A probable reaction scheme, by which the in situ EQCM and potentiometric data obtained may be reasonably explained, is as follows:

$$(Fc^\circ, n'S)_{poly} + (ClO_4^-)_{soln} + m'(S)_{soln} \rightleftarrows (Fc^+\cdot ClO_4^-, (n'+m')S)_{poly} + e^-, \quad (7)$$

where S represents the solvent (CH_3CN), the coefficients m' and n' are not necessarily integers as in Eq. 4.[10] The mechanism of the ion and solvent transport accompanying the redox reaction of the PVF film in acetonitrile media may be depicted schematically in the same manner as in Fig. 5. To our knowledge, this is a first report concerning the in situ EQCM behavior of PVF film in nonaqueous media.

In conclusion, the present study strongly demonstrates that a combination of the in situ EQCM measurement and the measurement of the dependence of $(E^f_{poly})_{app}$ on the electrolyte concentration allows us to elucidate quantitatively the ion and/or solvent transport process across the polymer film/solution interface accompanying the redox reaction of thin films on electrode surfaces.

This work was partially supported by a Grant-in-Aid for Scientific Research Nos. 02805096 and 01470064 from the Ministry of Education, Science and Culture.

References

1) For review; a) R. W. Murray, "Electroanalytical Chemistry," ed by A. J. Bard, Marcel Dekker, New York (1984), Vol. 13, p. 191. b) A. R. Hillman, "Electrochemical Science and Technology," ed by R. G. Linford, Elsevier Applied Science, Amsterdam (1987), p. 103. c) M. Kaneko and Wöhrle, "Advances in Polymer Science 84," Springer-Verlag, Berlin (1988), p 141. d) N. Oyama and T. Ohsaka, "Molecular Design of Electrode Surfaces," ed by R. W. Murray, John Wiely, in press.

2) a) N. Oyama, T. Ohsaka, M. Kaneko, and H. Matsuda, *J. Am. Chem. Soc.*, **105**, 6003 (1983). b) N. Oyama, T. Ohsaka, and T. Ushirogouchi, *J. Phys. Chem.*, **88**, 5274 (1984). c) T. Ohsaka, T. Okajima, and N. Oyama, *J. Electroanal. Chem.*, **215**, 191 (1986). d) N. Oyama, T. Ohsaka, H. Yamamoto, and M. Kaneko, *J. Phys. Chem.*, **90**, 3850 (1986). e) T. Ohsaka, H. Yamamoto, and N. Oyama, *J. Phys. Chem.*, **91**, 3775 (1987).

3) a) M. R. Deakin and D. A. Buttry, *Anal. Chem.*, **61**, 1147A (1989). b) D. A. Buttry, "Application of the Quartz Crystal Microbalance to Electrochemistry, Analytical Chemistry," ed by A. J. Bard, Marcel Dekker, New York (1991), Vol. 17, p. 1.

4) a) N. Oyama, N. Yamamoto, O. Hatozaki, and T. Ohsaka, *Jpn. J. Appl. Phys.*, **29**, L818 (1990). b) P. T. Varineau and D. A. Buttry, *J. Phys.*, **91**, 1292 (1987). c) M. D. Ward, *J. Phys. Chem.*, **92**, 2049 (1988). d) A. J. Kelly, T. Ohsaka, N. Oyama, R. J. Forster, and J. G. Vos, *J. Electroanal. Chem.*, **287**, 185 (1990). e) H. Daifuku, T. Kawagoe, N. Yamamoto, T. Ohsaka, and N. Oyama, *J. Electroanal. Chem.*, **274**, 313 (1989). f) W. H. Smyrl and K. Naoi, *AIChE Symp. Ser.*, **86**, 71 (1990). g) N. Yamamoto, T. Ohsaka, T. Terashima, and N. Oyama, *J. Electroanal. Chem.*, **296**, 463 (1990). h) S. Bruckenstein, C. P. Wilde, M. Shay, A. R. Hillman, and D. C. Loveday, *J. Electroanal. Chem.*, **258**, 457 (1989). i) A. R. Hillman, D. C. Loveday, and S. Bruckenstein, *J. Electroanal. Chem.*, **274**, 157 (1989). j) M. D. Ward, *J. Electroanal. Chem.*, **236**, 139 (1987).

5) a) R. Naegeli, J. Redepenning, and F. C. Anson, *J. Phys. Chem.*, **90**, 6227 (1986). b) J. Redepenning and F. C. Anson, *J. Phys. Chem.*, **91**, 4549 (1987). c) A. Fitch, *J. Electroanal. Chem.*, **284**, 237 (1990).

6) S. Bruckenstein and M. Shay, *Electrochim. Acta*, **30**, 1295 (1985).

7) G. Sauerbrey, *Z. Phys.*, **155**, 206 (1959).

8) T. W. Smith, J. E. Kuder, and D. Wychik, *J. Polym. Sci., Polym. Chem. Ed.*, **14**, 2433 (1976).

9) a) R. A. Robinson and R. H. Stokes, "Electrolyte Solutions," 2nd ed, Butterworth, London (1970). b) H. S. Harned and B. B. Owen, "The Physical Chemistry of Electrolytic Solutions," 3rd ed, ACS Monograph Series, No. 137, Reinhold, New York (1957).

10) S. Bruckenstein and A. R. Hillman, *J. Phys. Chem.*, **92**, 4837 (1988).

11) The F_c°/F_c^{+} couple in the PVF film and the $F_c\text{-}N^{+}/F_c\text{-}N^{2+}$ couple are similar in their molecular structures. It is, if possible, preferable that the charges on the oxidized and reduced forms of the PVF film are the same as those of the solution-phase ferrocene compound (as in the case of the acetonitrile solution system). However, the solubility of the reduced form of ferrocene (F_c°) in the aqueous solutions used was too low to conduct usual electrochemical experiments, so that the water-soluble ferrocene derivative (i.e., $F_c\text{-}N^{+}$) was employed in this study.